Radiation on Conducting Sphere and Hemispherical Bulge in Conducting Plane: Further Development

N.F. Shul'ga[1], *V.V. Syshchenko*[2]

[1]*NSC KIPT, Kharkov, Ukraine*

[2]*Belgorod National Research University, Russian Federation*

Diffraction radiation (**DR**) as well as the transition radiation (**TR**) of a charge on a perfectly conducting sphere had been studied in

- N.F. Shul'ga, V.V. Syshchenko, E.A. Larikova // Nucl. Instrum. Meth. B **402** (2017) 167 (Proceedings of Channeling-2016).

using the method of images known from electrostatics. In the paper

- V.V. Syshchenko, E.A. Larikova, Yu.P Gladkih // JINST **12** (2017) C12057 (Proceedings of RREPS-2017).

DR on the hemispherical bulge in a perfectly conducting plane had been considered using the same approach.

Here we shall discuss three topics:

1. Polarization of DR on the sphere as well as on the hemispherical bulge
2. TR on the hemispherical bulge
3. Coherent radiation from a bunch of charged particles

Previously we shall briefly describe our approach.

One of the ways to describe these types of radiation is the application of the boundary conditions to the Maxwell equations solutions for the field of the moving particle in two media. It becomes evident that the boundary conditions could be satisfied only after addition the solution of free Maxwell equations that corresponds to the radiation field.

The conditions on the boundary between vacuum and perfect conductor could be satisfied in some cases via introduction of one or more fictitious charges along with the real charged particle; this approach to electrostatic problems is known as the method of images, see, e.g.,

J.D. Jackson, *Classical Electrodynamics*, Wiley, New York, 1999.

Namely the method of images had been used in the pioneering paper

V.L. Ginzburg, I.M. Frank // J. Phys. USSR 9 (1945) 353.

where TR on a metal plane had been predicted. The method of images had been used also in

G.A. Askaryan // JETP 29 (1955) 388 *(in Russian)*.

for consideration of TR under passage of the particle through the center of the perfectly conducting sphere in dipole approximation. The authors of

A.C. Amatuni, A.M. Oganesyan // Izv. Akad. Arm. SSR, XIV, No. 5 (1961) 99 *(in Russian)*.

used that approach for description of DR on the sphere, however, also in dipole approximation that leads to overestimation of the effect.

Method of images in DR description

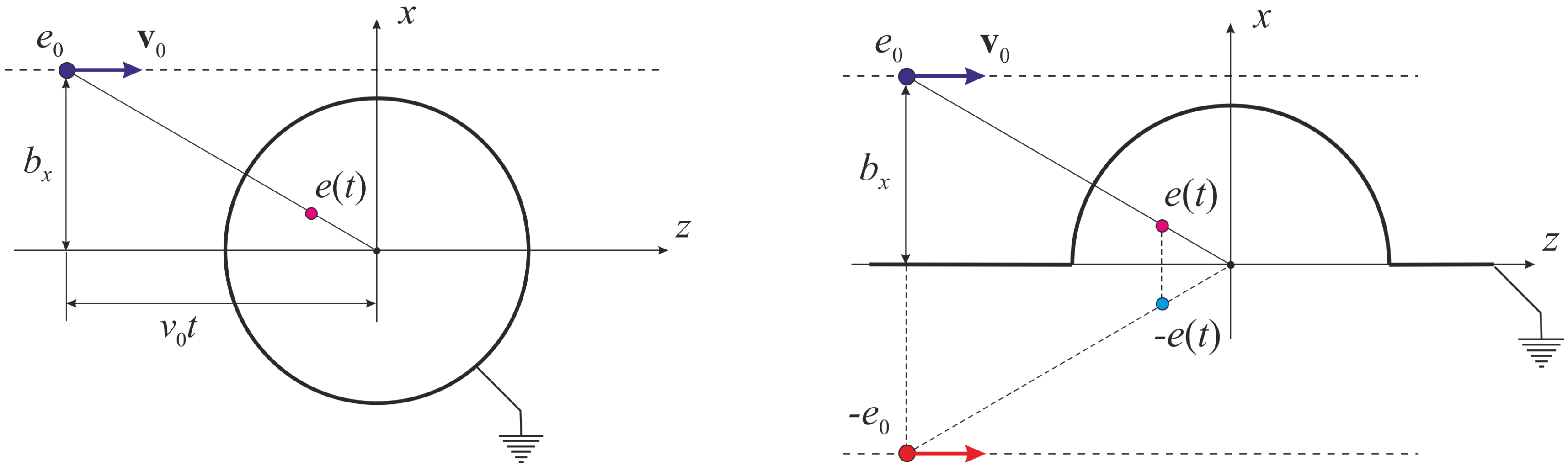

Consider the real charge e_0 passing by the grounded conducting sphere of the radius R. Its "image" $e(t)$ has to be placed in the inverse conjugated point with coordinates $x(t)$, $y(t)$, $z(t)$:

$$e(t) = -e_0\frac{R}{\sqrt{b^2 + v_0^2t^2}}, \quad x(t) = \frac{R^2 b_x}{b^2 + v_0^2t^2}, \quad y(t) = \frac{R^2 b_y}{b^2 + v_0^2t^2}, \quad z(t) = \frac{R^2 v_0 t}{b^2 + v_0^2t^2}, \quad b = \sqrt{b_x^2 + b_y^2}.$$

So, while the incident particle moves uniformly, the "image" $e(t)$ will move accelerated. The radiation produced by non-uniform motion of the fictitious charge will be described by well-known formula

$$\frac{d\mathcal{E}}{d\omega d\Omega} = \frac{1}{4\pi^2 c}\left|[\mathbf{k},\mathbf{I}]\right|^2 = \frac{1}{4\pi^2 c}\left\{\mathbf{k}^2|\mathbf{I}|^2 - |\mathbf{k}\cdot\mathbf{I}|^2\right\}, \qquad \mathbf{I} = \int_{-\infty}^{\infty} e(t)\,\mathbf{v}(t)\,e^{i(\omega t - \mathbf{kr}(t))}\,dt$$

In the case of hemispherical bulge on a conducting plane we have three "images", two of which, $e(t)$ and $-e(t)$, move accelerated.

The integrands are smooth functions, and the integration can be easily performed numerically, that leads to the spectral-angular density of diffraction radiation in the form

$$\frac{d\mathcal{E}}{d\omega d\Omega} = \frac{e_0^2}{4\pi^2 c}\,\Phi_{DR}(\theta,\varphi,\omega),$$

where the angular distribution $\Phi_{DR}(\theta, \varphi, \omega)$ looks as follows:

DR on sphere:

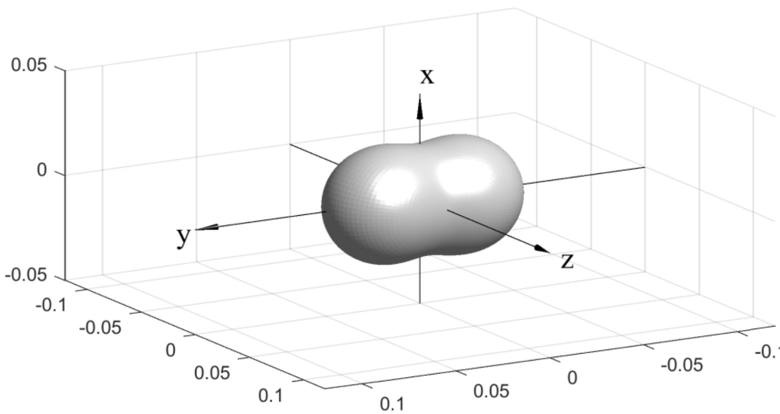

DR on hemisphere:

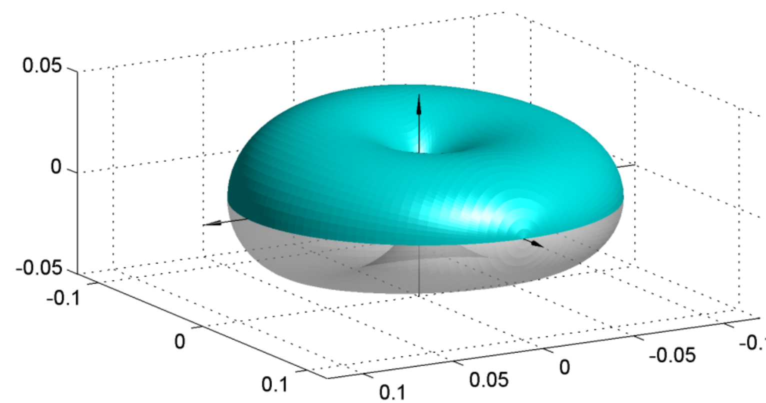

The angular dependence as direction diagram of DR intensity on the sphere (*left*) and hemisphere (*right*) for the passage of the real charge under $b_x = R+0$ and $b_y = 0$ (sliding incidence, when DR intensity is maximal for the whole range of wavelengths) and $R\omega/v_0 = 2.4$ (this choice is due to the maximum of DR on hemisphere spectrum (see below) falls on $\omega b/v_0$? 2.4 and $b = R$ in the given case). This shape of the directional diagram is typical; for higher frequencies the slight forward-backward asymmetry increases.

In non-relativistic ($v_0 << c$) and low-frequency ($\boxed{?} << cb / R^2$ or $\boxed{?} >> 2\boxed{?}R^2 / b$) case we can neglect the values marked yellow in the **I** formulae:

$$I_x = 2e_0 bR^3 v_0^2 \frac{b_x}{b} \int_{-\infty}^{\infty} \exp\left\{ i \left[\omega t - \frac{(k_x b_x + k_y b_y)R^2}{b^2 + v_0^2 t^2} - \frac{k_z R^2 v_0 t}{b^2 + v_0^2 t^2} \right] \right\} \frac{t\,dt}{(b^2 + v_0^2 t^2)^{5/2}},$$

$$I_y = 2e_0 bR^3 v_0^2 \frac{b_y}{b} \int_{-\infty}^{\infty} \exp\left\{ i \left[\omega t - \frac{(k_x b_x + k_y b_y)R^2}{b^2 + v_0^2 t^2} - \frac{k_z R^2 v_0 t}{b^2 + v_0^2 t^2} \right] \right\} \frac{t\,dt}{(b^2 + v_0^2 t^2)^{5/2}},$$

$$I_z = -e_0 R^3 v_0 \int_{-\infty}^{\infty} \exp\left\{ i \left[\omega t - \frac{(k_x b_x + k_y b_y)R^2}{b^2 + v_0^2 t^2} - \frac{k_z R^2 v_0 t}{b^2 + v_0^2 t^2} \right] \right\} \frac{(b^2 - v_0^2 t^2)\,dt}{(b^2 + v_0^2 t^2)^{5/2}}.$$

for DR on the sphere that gives

$$I_x \approx \frac{4}{3} e_0 R^3 \frac{\omega^2}{v_0^2}\, iK_1\left(\frac{\omega}{v_0} b\right) \frac{b_x}{b}, \quad I_y \approx \frac{4}{3} e_0 R^3 \frac{\omega^2}{v_0^2}\, iK_1\left(\frac{\omega}{v_0} b\right) \frac{b_y}{b},$$

$$I_z \approx -\frac{4}{3} e_0 R^3 \frac{\omega^2}{v_0^2} K_0\left(\frac{\omega}{v_0} b\right) - \frac{2}{3} e_0 R^3 \frac{\omega}{v_0 b} K_1\left(\frac{\omega}{v_0} b\right)$$

and

$$I_x = 4e_0 b_x R^3 v_0^2 \int_{-\infty}^{\infty} \frac{t}{(b^2+v_0^2t^2)^{5/2}} \exp\left\{i\left[\omega t - \frac{k_y b_y R^2}{b^2+v_0^2t^2} - \frac{k_z R^2 v_0 t}{b^2+v_0^2t^2}\right]\right\} \cos\frac{k_x b_x R^2}{b^2+v_0^2t^2}\, dt,$$

$$I_y = -4ie_0 b_y R^3 v_0^2 \int_{-\infty}^{\infty} \frac{t}{(b^2+v_0^2t^2)^{5/2}} \exp\left\{i\left[\omega t - \frac{k_y b_y R^2}{b^2+v_0^2t^2} - \frac{k_z R^2 v_0 t}{b^2+v_0^2t^2}\right]\right\} \sin\frac{k_x b_x R^2}{b^2+v_0^2t^2}\, dt,$$

$$I_z = 2ie_0 R^3 v_0 \int_{-\infty}^{\infty} \frac{b^2-v_0^2t^2}{(b^2+v_0^2t^2)^{5/2}} \exp\left\{i\left[\omega t - \frac{k_y b_y R^2}{b^2+v_0^2t^2} - \frac{k_z R^2 v_0 t}{b^2+v_0^2t^2}\right]\right\} \sin\frac{k_x b_x R^2}{b^2+v_0^2t^2}\, dt.$$

for DR on the hemispherical bulge that gives

$$I_x \approx \frac{8}{3} e_0 R^3 \frac{\omega^2}{v_0^2}\, iK_1\left(\frac{\omega}{v_0} b\right) \frac{b_x}{b}, \quad I_y \approx I_z \approx 0$$

This approximation is rather good, as we can see comparing the numerical spectra and the approximated analytical ones:

Spectral density of DR on the sphere (upper panel) and hemisphere (lower panel) under $b_y = 0$ and $b_x = R + 0$ calculated using analytical formula (blue curve) and via numerical integration (red circles). Dashed curve presents the dipole result by Amatuni and Oganesyan.

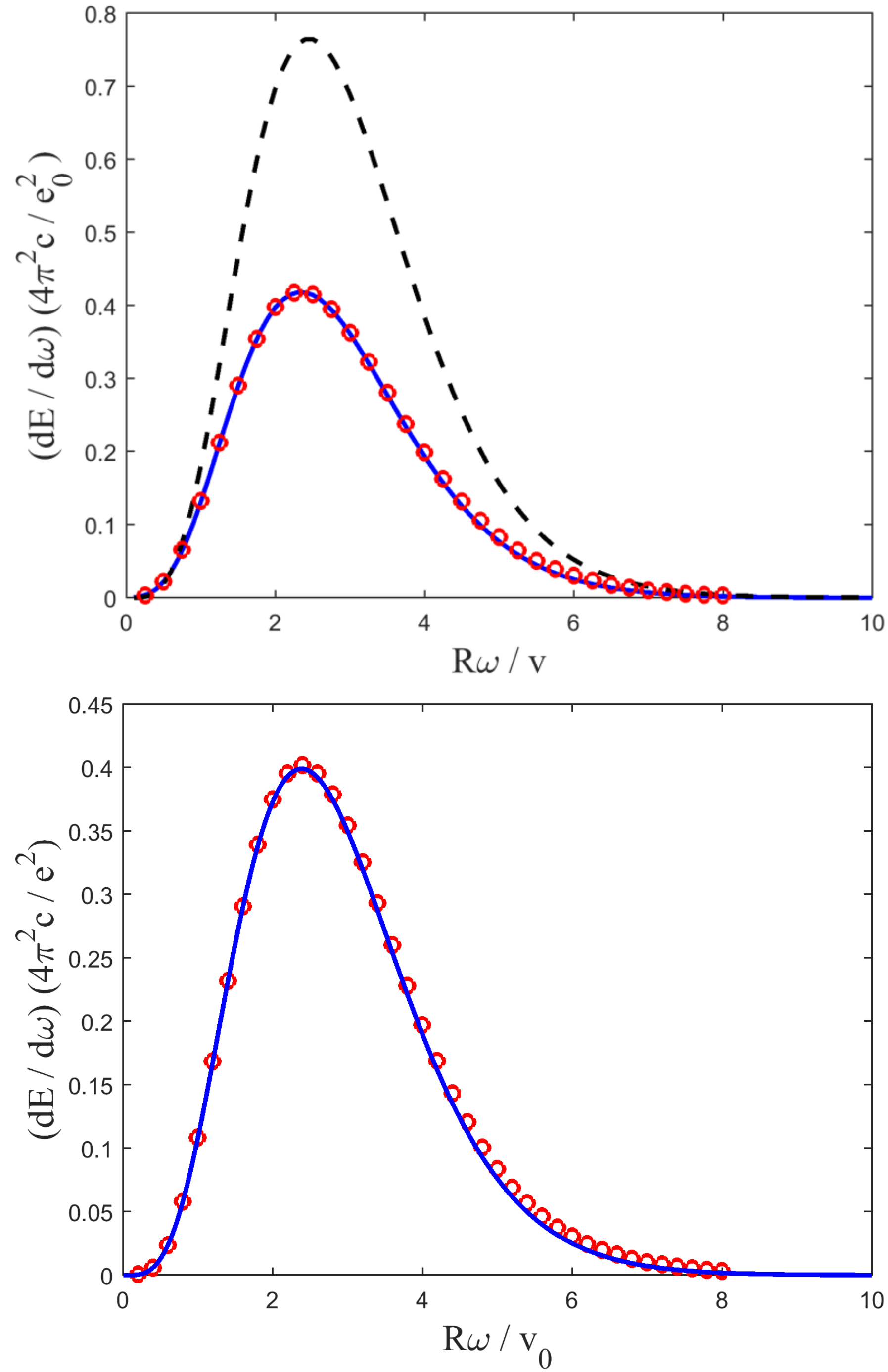

DR polarization on the sphere

Choosing two polarization vectors $\mathbf{e}_1 \perp \mathbf{e}_2 \perp \mathbf{k}$ and calculating the scalar products $(\mathbf{e}_1 \cdot \mathbf{I})$ and $(\mathbf{e}_2 \cdot \mathbf{I})$, we can obtain the Stokes parameters and hence the complete information about the radiation polarization. We found that the radiation is 100% polarized with the following characteristics for different radiation angles:

circular polarization

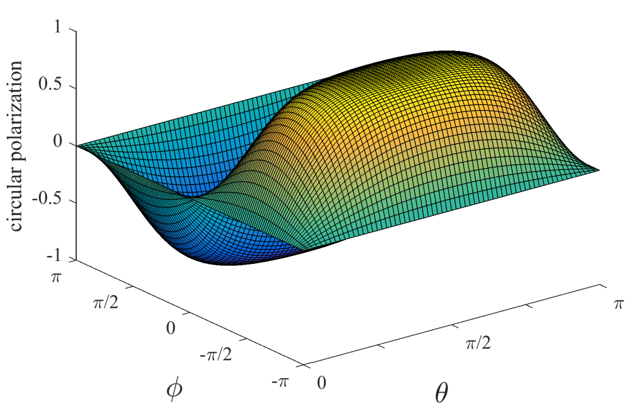

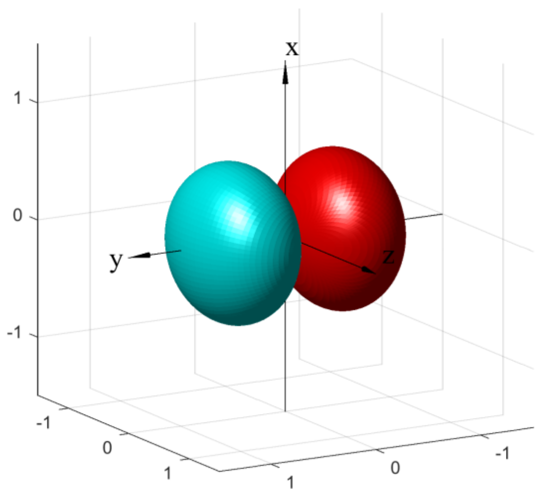

linear polarization

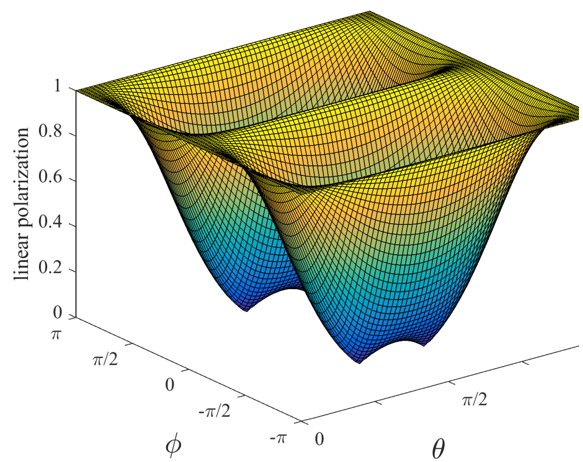

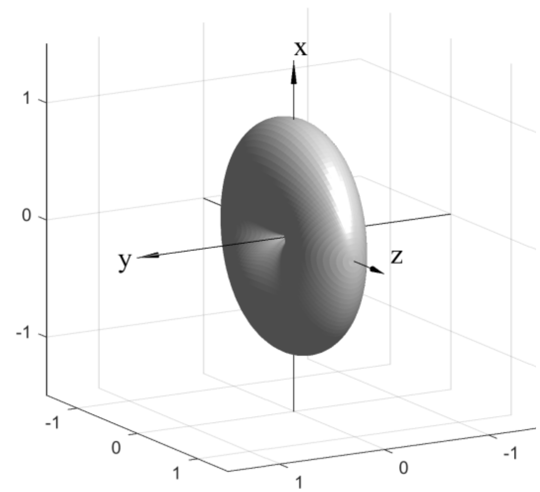

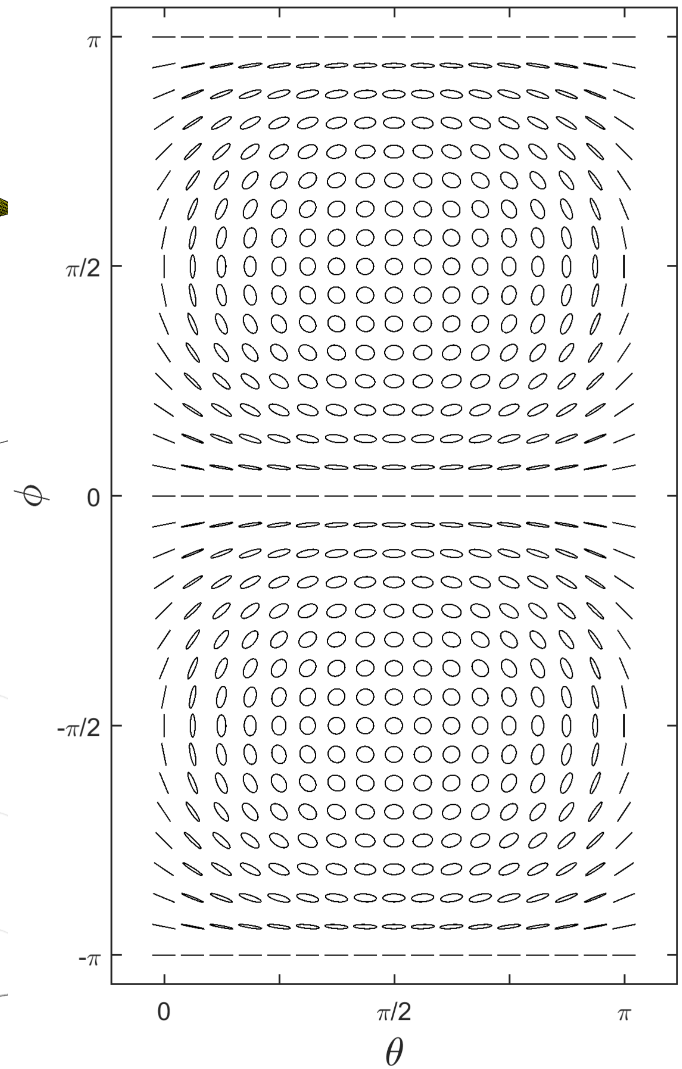

DR polarization on the sphere

Here we mark the points of 100% circular polarization (colored) and 100% linear polarization (black belt) on the radiation intensity directional diagram. Note that the directional diagram's symmetry plane (as well as the plane of 100% linear polarization) is the plane that contains the center of the sphere and the incident particle's trajectory. So, the directional diagram rotates around *z* axis with the incident particle's trajectory:

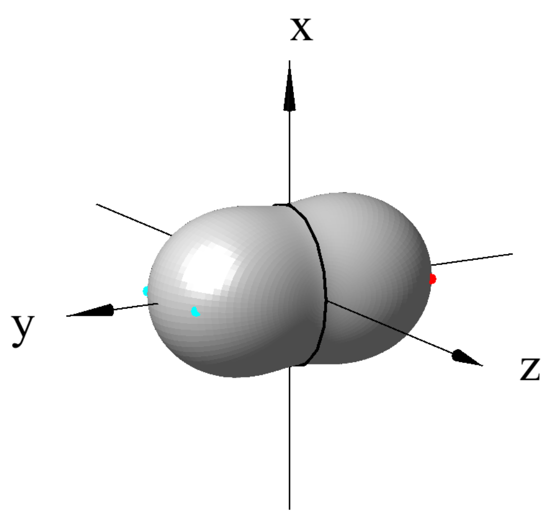

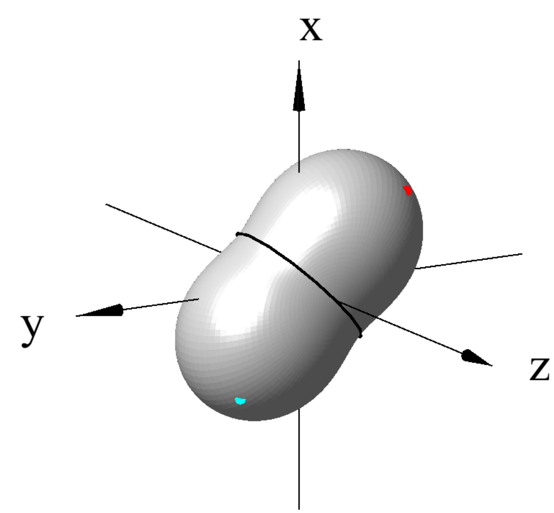

$b_x = R+0$ and $b_y = 0$ $\qquad$ $b_x = b_y = R/\sqrt{2} + 0$

That opens the possibility to detect the relation between the components b_x and b_y of the 2-dimentional impact parameter of the incident particle using the polarization-sensitive detector:

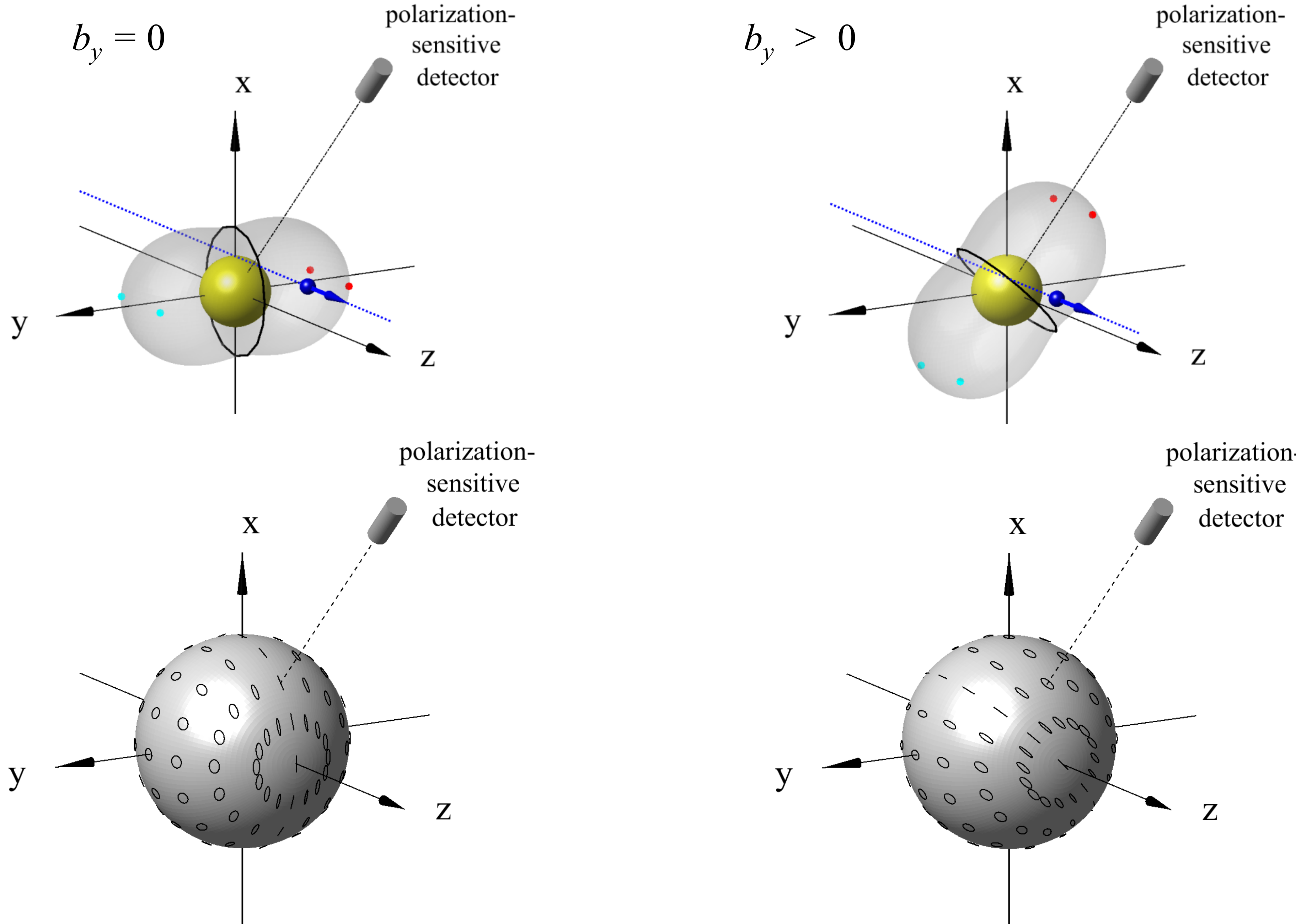

In the case $b_y = 0$ we detect 100% linear polarization while in the case $b_y > 0$ or $b_y < 0$ we detect elliptical polarization, left or right.

DR polarization on the hemispherical bulge

This situation is simple: the radiation is linearly polarized in the plane that contains the vectors $\mathbf{k}$ and $\mathbf{e}_x$:

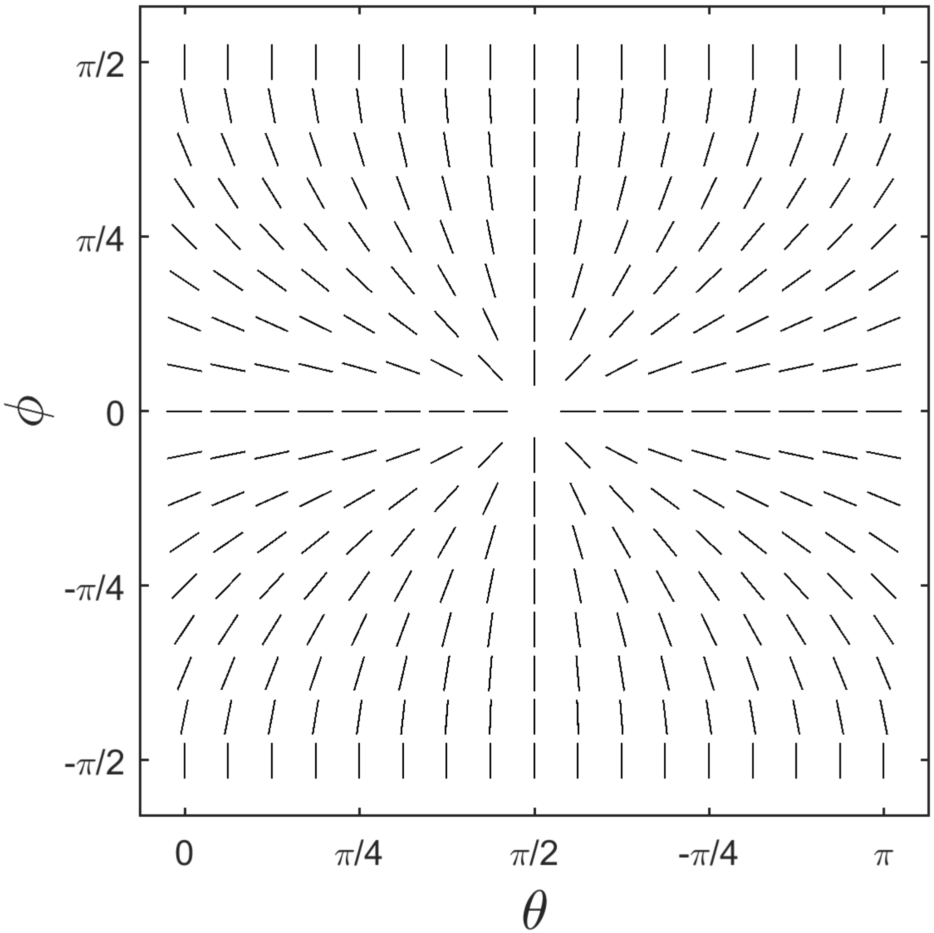

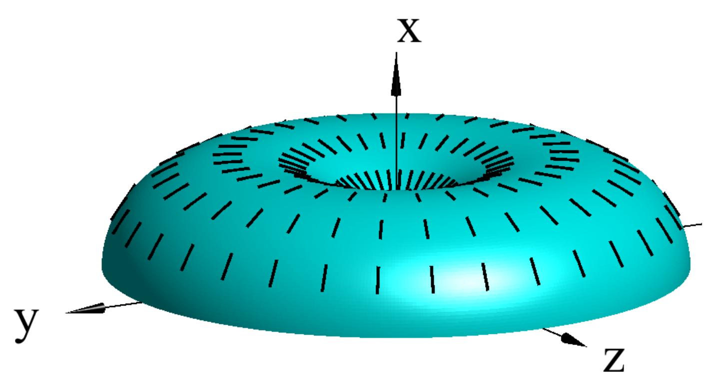

TR on the hemispherical bulge

Transition radiation changes the diffraction one when the incident particle's trajectory crosses the target boundary. The simplest manifestation of TR production is the origin of the radiation in the hard range of the spectrum:

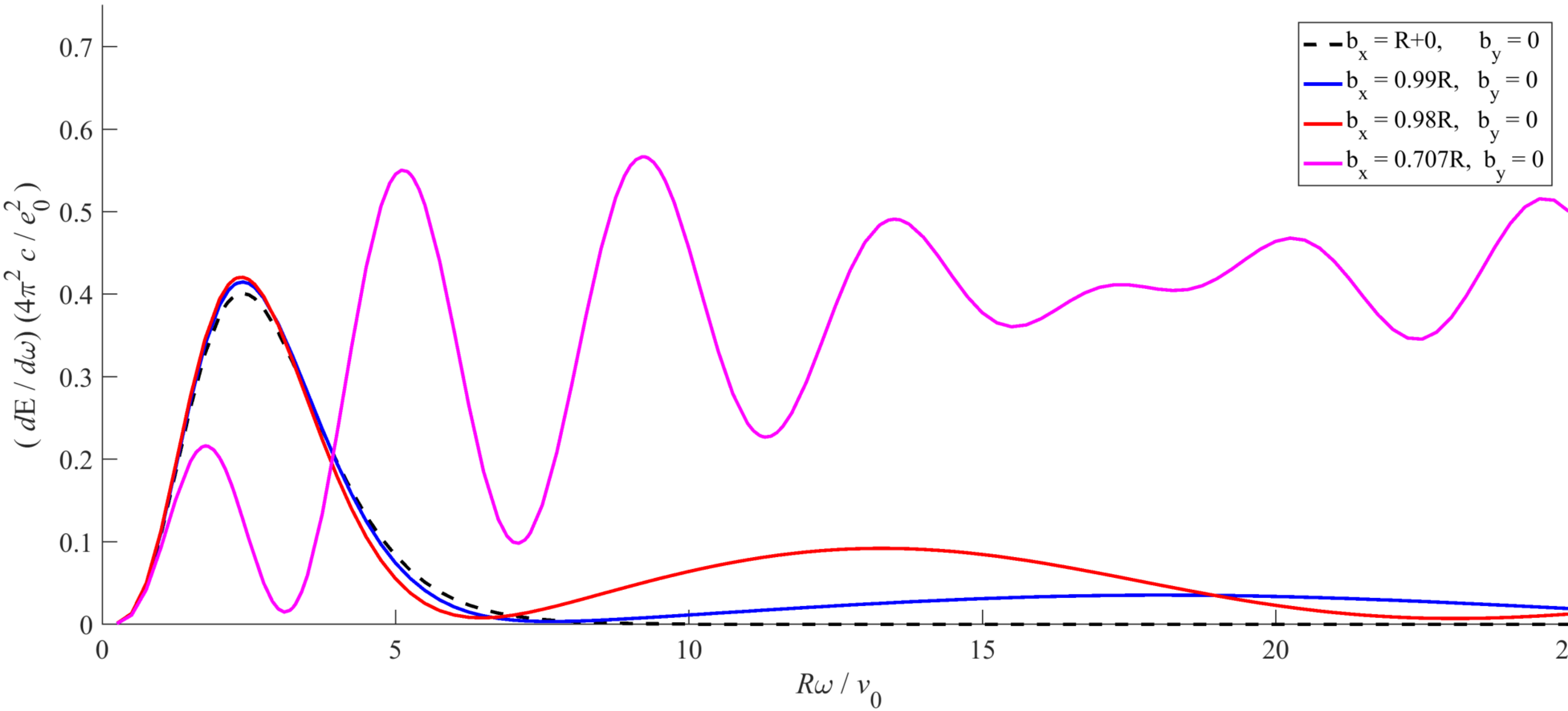

TR on sphere vs hemisphere…

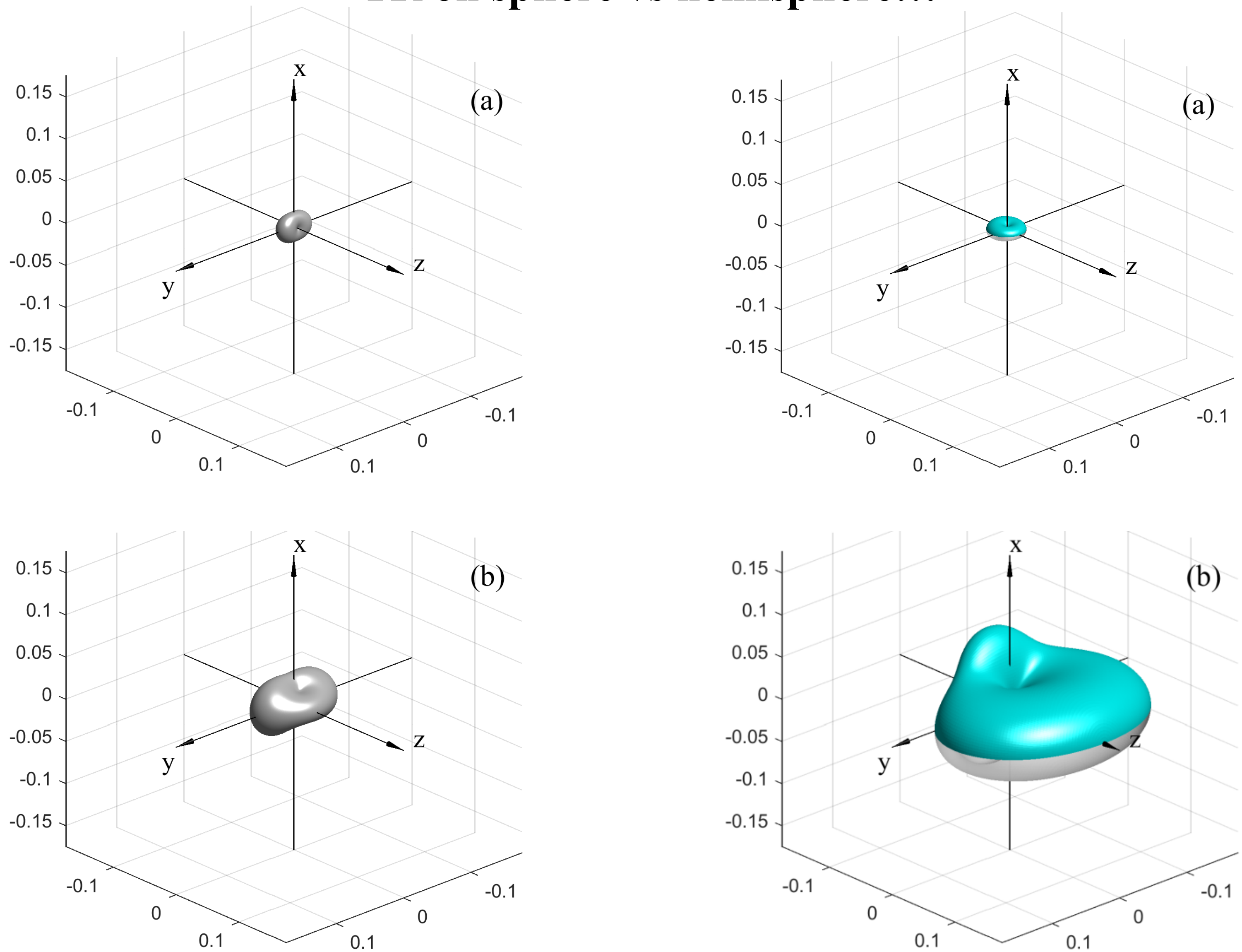

Directional diagrams for TR on the sphere (left) vs hemisphere (right), $v_0 = 0.1c$,
$b_x = R/\boxed{?}2$, $b_y = 0$, $R\boxed{?}/v_0 = 1$ (a), 10 (b).

TR on sphere vs hemisphere…

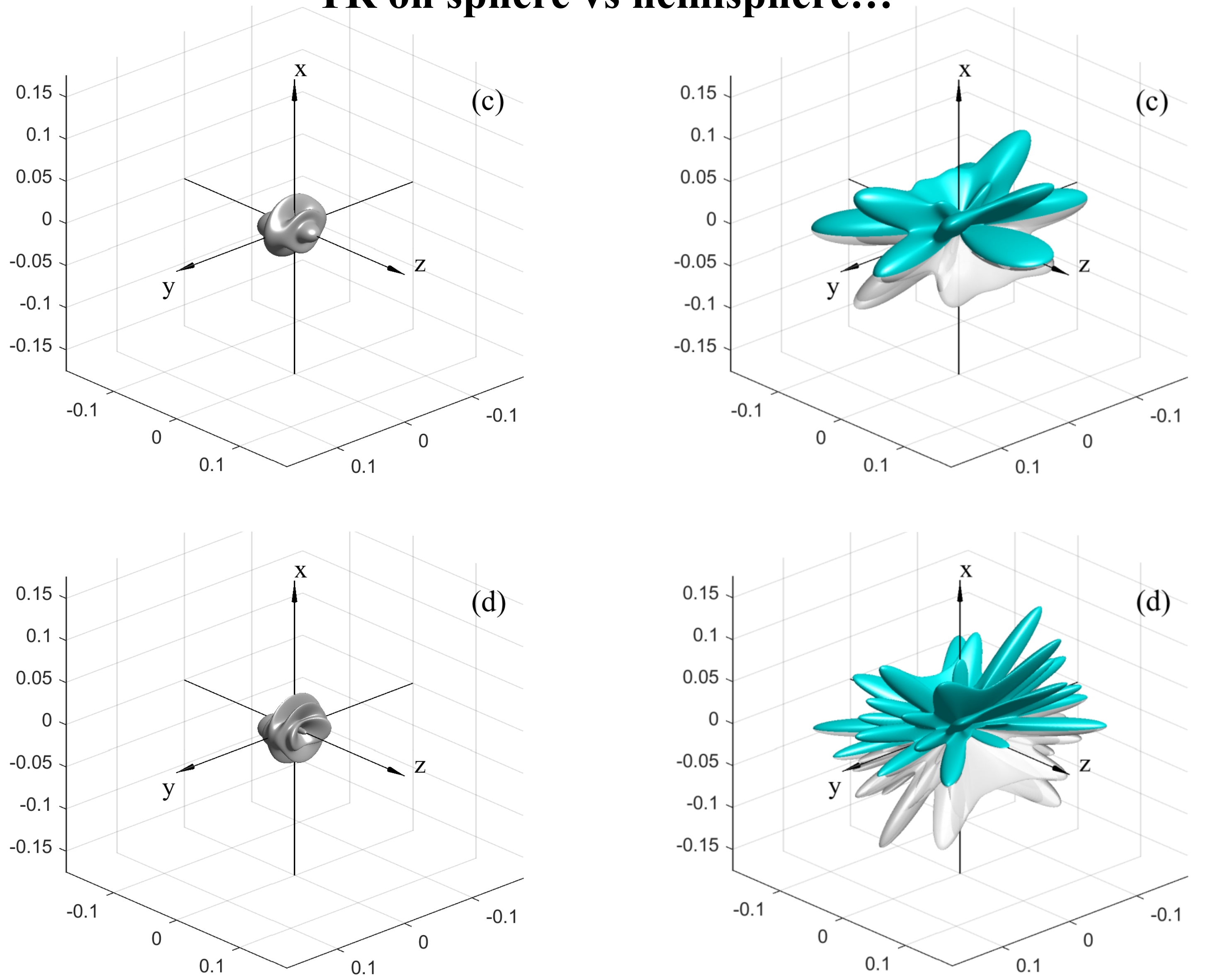

Directional diagrams for TR on the sphere (left) vs hemisphere (right), $v_0 = 0.1c$, $b_x = R/\boxed{?}\,2$, $b_y = 0$, $R\boxed{?}/v_0 = 50$ (c), 100 (d).

TR on sphere vs hemisphere…

Complex character of interference of the contributions from 4 charges leads to just more sophisticated angular distribution of TR on the hemispherical bulge than on the sphere:

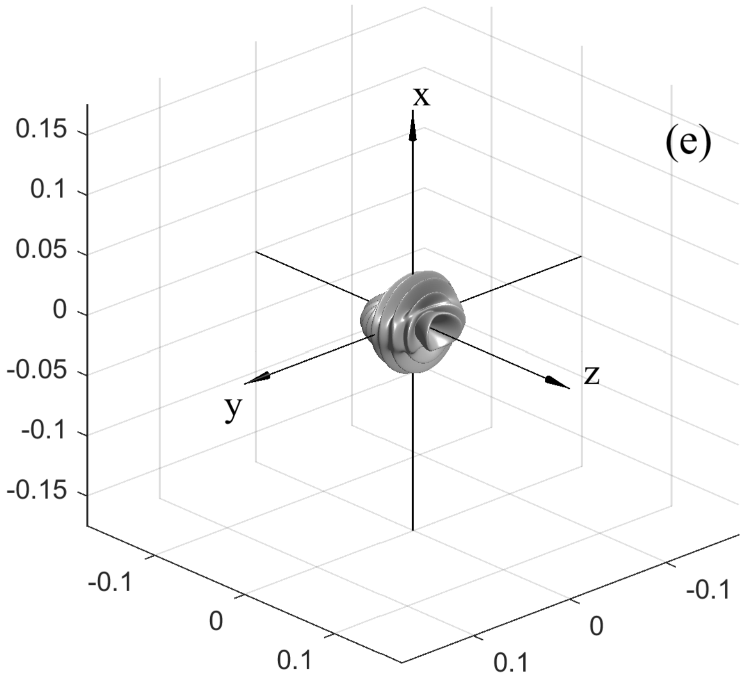

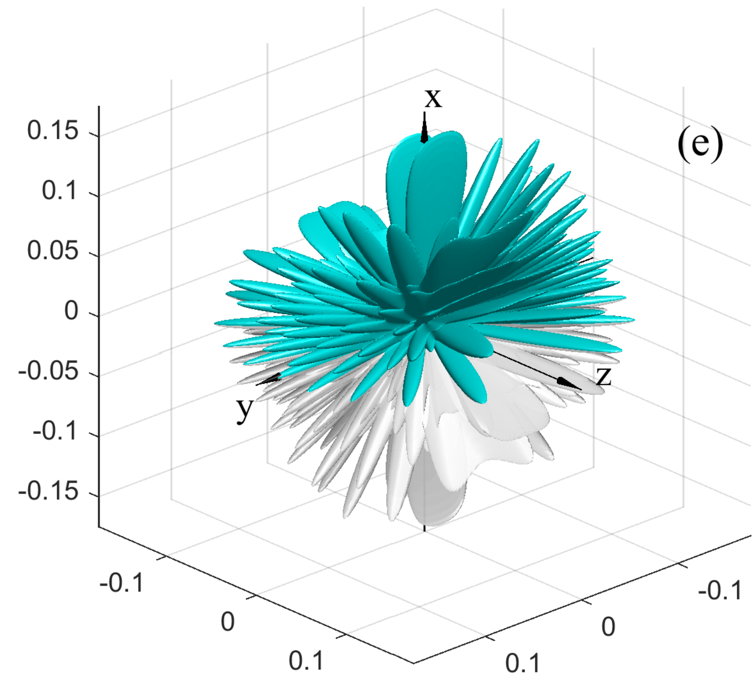

TR on the sphere (left) vs hemisphere (right), $v_0 = 0.1c$, $b_x = R/\boxed{?}2$, $b_y = 0$, $R\boxed{?}/v_0 = 200$.

Note that in the high frequency domain the transverse size of the particle's Coulomb field $v_0/\boxed{?} \ll R$ that permits to neglect the metal surface curvature. But in this case we can extend our approach to relativistic incident particle!

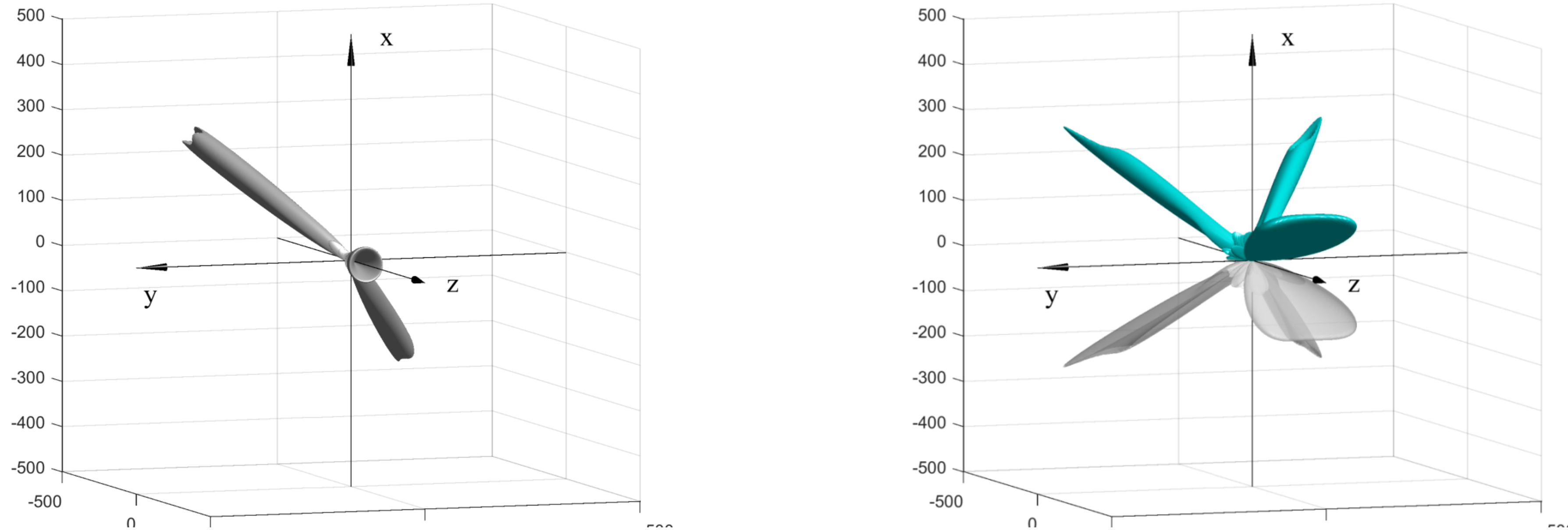

Relativistic case: $b_y = b_x = 0.2706R$ (that is sin(⍰/8) /⍰2), $R\omega/v_0 = 20$, $v_0 = 0.999c$.

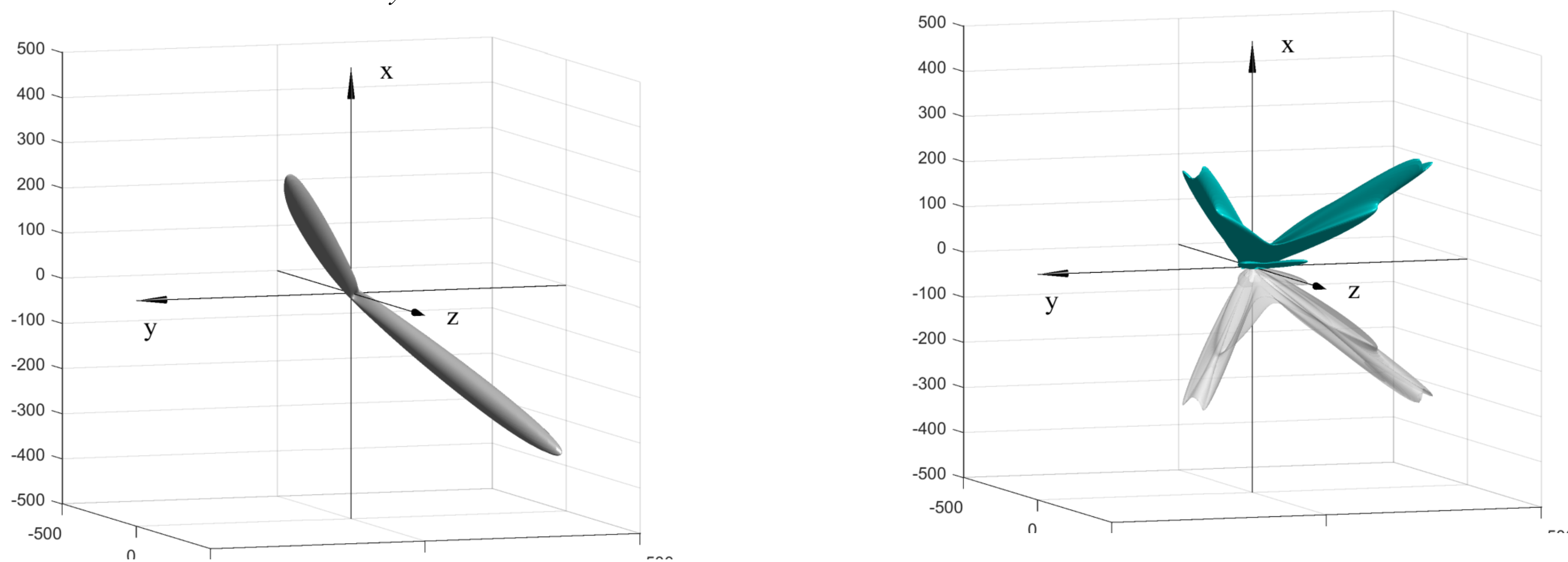

The same for $b_y = b_x = 0.6533R$ (that is sin(3⍰/8) /⍰2).

TR on hemisphere, ultrarelativistic case: $v_0 = 0.9999c$, $R\omega/v_0 = 20$,
$b_y = b_x = \sin(?/8)$ / ?2 (left), $b_y = b_x = \sin(3?/8)$ / ?2 (right).

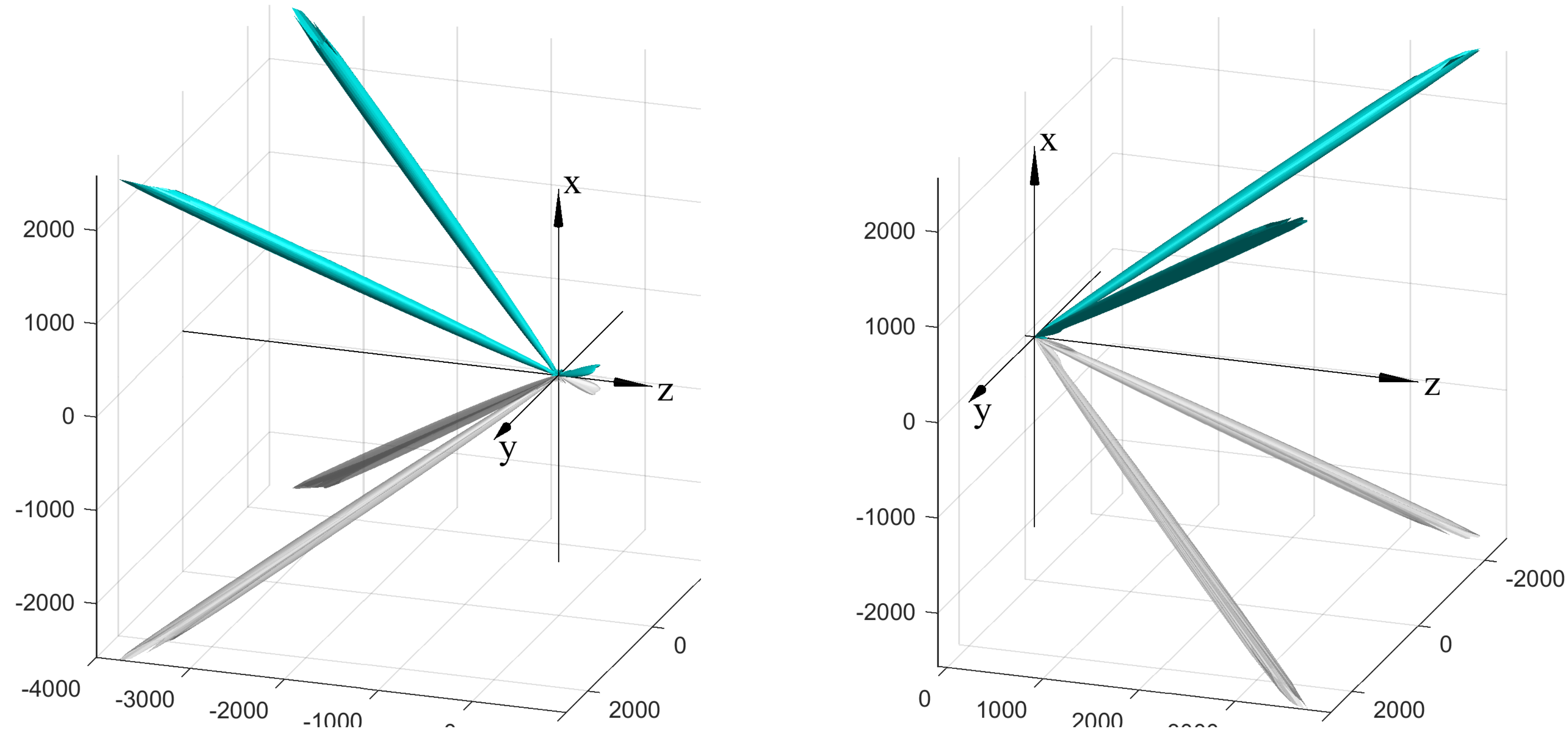

The genesis of these pictures is rather clear: each charge, real or fictitious, produces under the interaction with the metal surface the typical TR cone of radiation in its forward direction. However, the radiation in the z direction is suppressed here due to destructive interference of the corresponding contributions.

DR from a bunch of incident particles on the hemisphere

Of course, the radiation from the bunch could be calculated numerically, but here we consider two situations that permit simple analytical solution.

1. "Pencil"-bunch with charge density distribution along the direction of incidence

$$N\, n(z'), \quad \text{where} \quad \int_{-\infty}^{\infty} n(z')\, dz' = 1\,,$$

N is the total number of particles in the bunch, *z'* is the coordinate in the internal bunch frame. In this case we obtain the spectral-angular distribution of the radiation from the bunch in the form

$$\frac{d\mathcal{E}}{d\omega d\Omega} = \left(\frac{d\mathcal{E}}{d\omega d\Omega}\right)_1 N^2 \left|F_{\|}\left(\frac{\omega}{v_0}\right)\right|^2, \quad \text{where} \quad F_{\|}\left(\frac{\omega}{v_0}\right) = \int_{-\infty}^{\infty} n(z') \exp\left(-i\frac{\omega}{v_0} z'\right) dz'$$

Note that the charge distribution in the pencil bunch has no influence on the shape of the radiation angular distribution, only the total intensity under given frequency depends on it.

DR from pencil bunch on the hemisphere

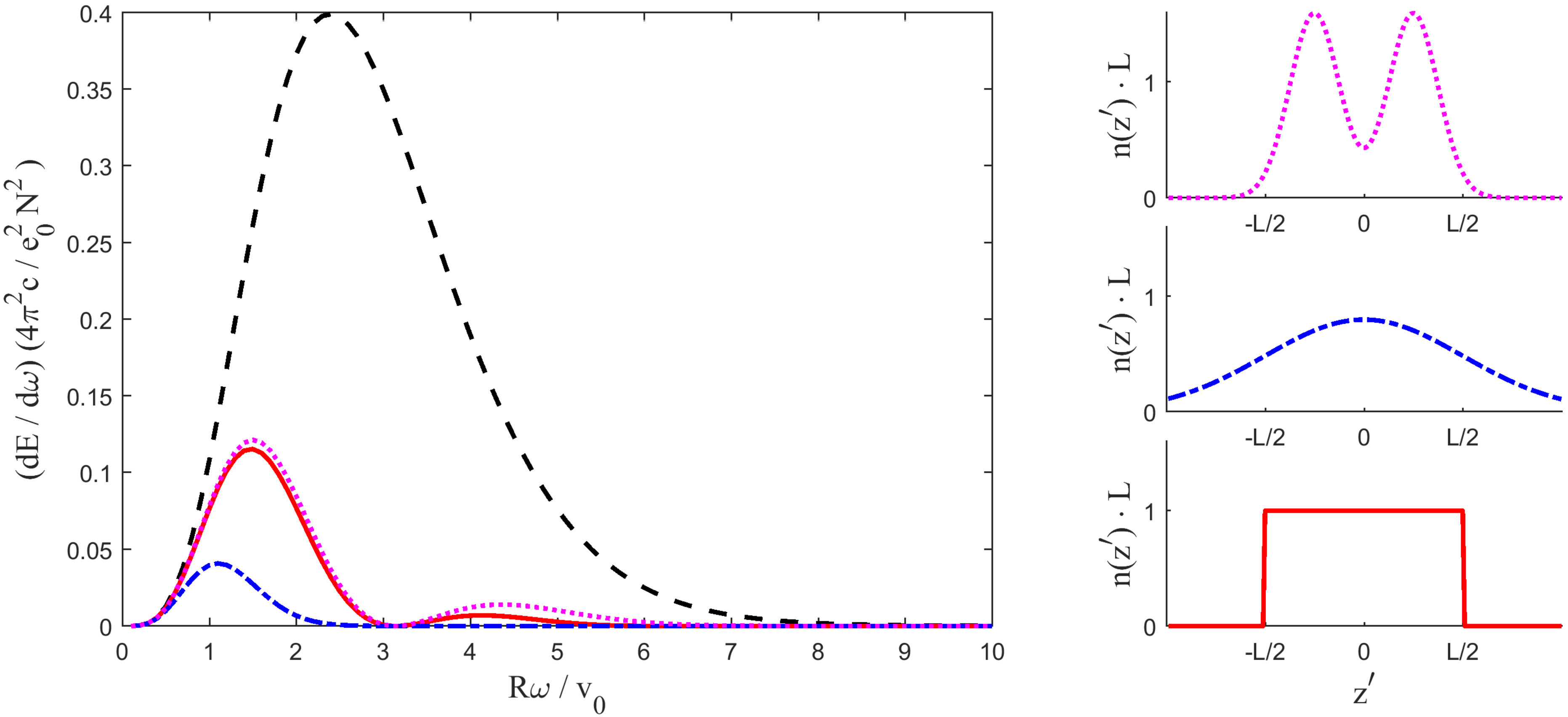

Spectrum of DR from the pencil bunch with uniform (red), Gaussian (blue) and double Gaussian (magenta) density for $L = 2R$. Dashed line corrsponds to the point charge.

2. Another situation that permits simple analytical solution is the uniform "pencil"-bunch oriented along y axis with the length $L_y >> R$:

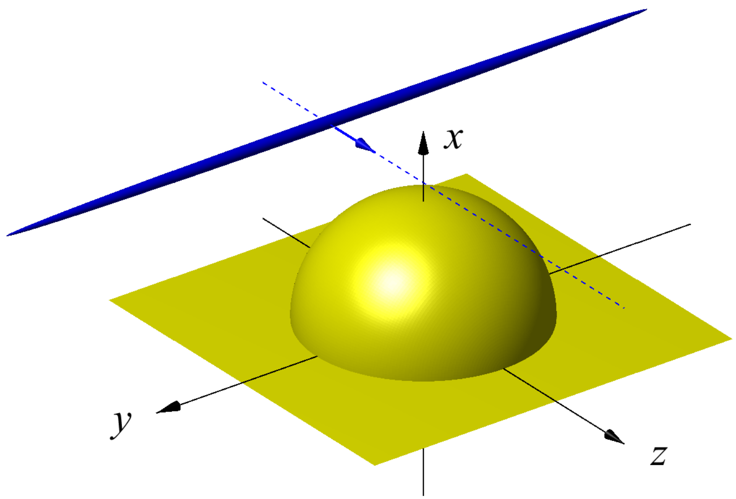

$$I_x = \frac{N}{L_y} \frac{8\pi}{3} e_0 R^3 \frac{\omega}{v_0} i \exp\left(-\frac{\omega}{v_0} b_x\right)$$

Here we obtain simple exponential dependence of the radiation intensity on the impact parameter, also without influence on the angular distribution shape:

$$\frac{d\mathcal{E}}{d\omega d\Omega} = \frac{1}{4\pi^2 c} |\mathbf{k} \times \mathbf{e}_x|^2 \ |I_x|^2 =$$

$$= \left(\frac{N}{L_y}\right)^2 \frac{16}{9} e_0^2 \frac{\omega^4 R^6}{c^3 v_0^2} \exp\left(-2\frac{\omega}{v_0} b_x\right) (1 - \sin^2\theta \cos^2\varphi)$$

This result can be easily generalized to the case of wide charge distribution in the bunch along x axis.

THANK YOU FOR YOUR ATTENTION!

Concluding remarks #1: Range of validity

The perfect conductor approximation means the possibility of the metal's electrons instantly trace out the changes of the external electric field to meet the requirement of zero tangential component of the electric field on the metal surface. It is valid for the frequencies less than the inverse relaxation time $?^{-1}$ for the electrons in the metal. For instance, $?^{-1} = 5?10^{-13}$ s^{-1} for copper, so the results obtained surely could be applied up to THz and far infrared range.

On the other hand, Ginzburg and Tsytovich say:

"In fact, for the frequencies not higher the optic ones a good metal mirror (e.g. copper or silver) is rather close to the ideal one."

This means the applicability of the method of images also in the visible domain.

However, the surface plasma oscillations also could be important here that needs further investigation.

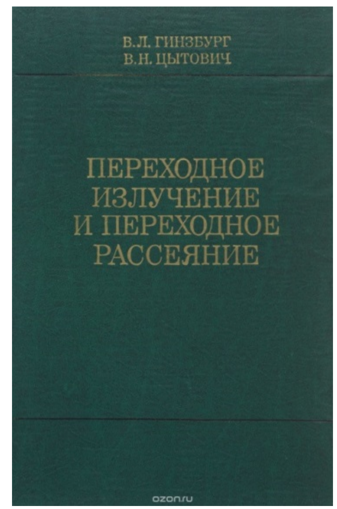

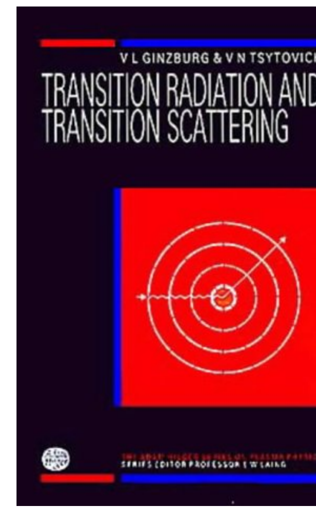

V.L. Ginzburg and V.N. Tsytovich, *Transition Radiation and Transition Scattering*, Nauka, Moscow, 1984 (*in Russian*); Adam Hilger, New York–London, 1990 (*in English*).

Concluding remarks #2: What can we do in relativistic case?

The difficulty lies in the geometric nature of the method of images: we can fit the fictive charge to meet the zero boundary condition on the sphere for the simple Coulomb field of slow incident particle, but not for the relativistically compressed one.

The only possibility to do something in relativistic case is to consider the high frequency limit, where the characteristic size of the Coulomb field, v_0?/?, is much smaller than the sphere radius *R*. Here we can neglect the metal surface curvature and consider the reflection of the incident field in the locally plane mirror.

However, we have a difficulty also in this case: the kinematic velocity of the fictive charge is not consistent with the degree of the relativistic compression of the Coulomb field of the incident particle. The resulting discrepancy in Lorentz factor values of the real and fictive charges is negligibly small only for the impact parameters extremely close to the sphere radius, $b = R+0$, namely

$$1 - R / (b^2 + v_0^2 t^2)^{1/2} \ll \boxed{?}^{-2} / 4 \text{ has to be…}$$

On this part of the trajectory the Loretz-factors are close together. Due to the constant acceleration of the fictive charge we expect synchrotron-like radiation.

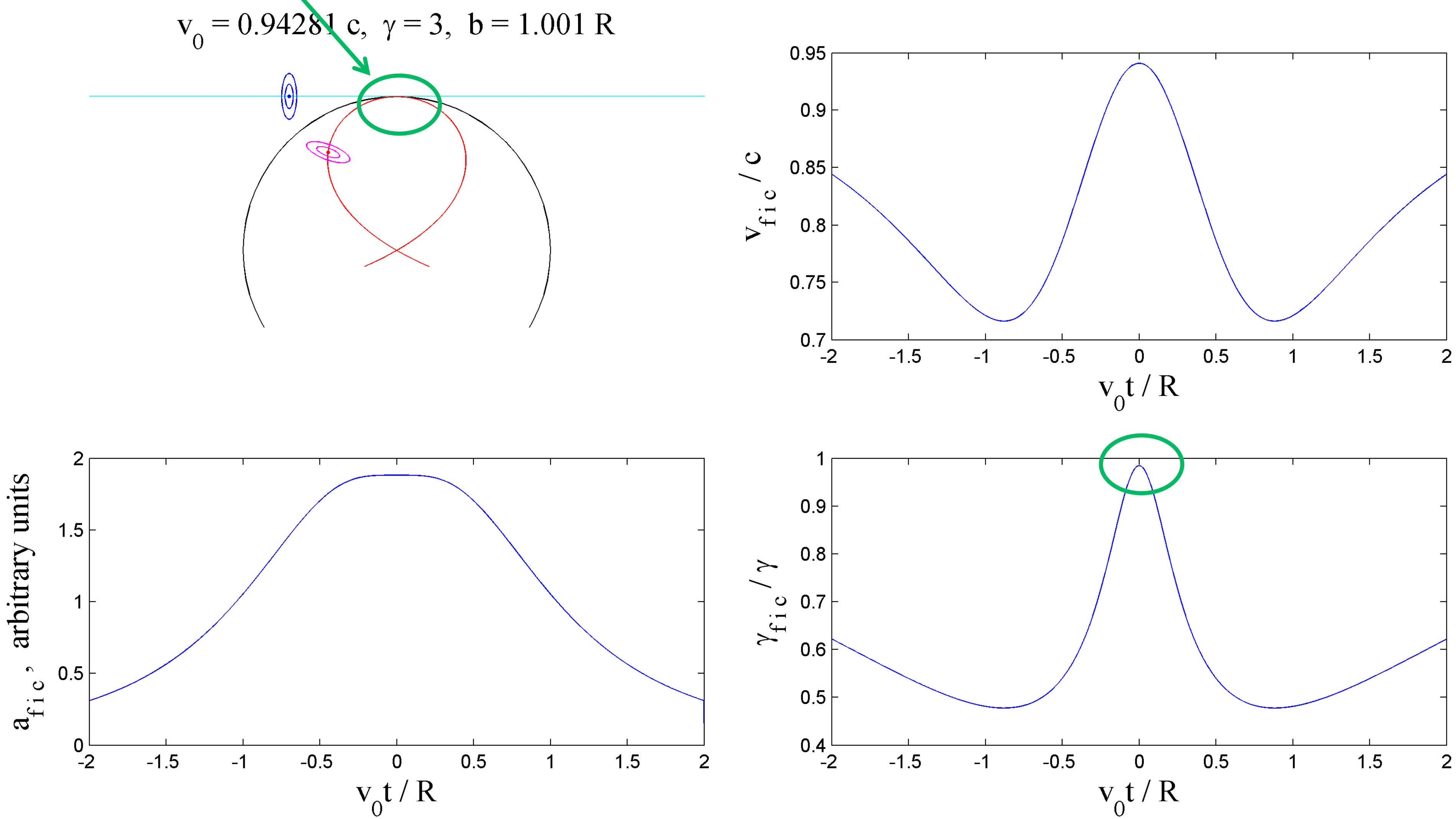

Summary:

- The radiation emitting under interaction of non-relativistic particle with a hemispheric bulge in the perfectly conducting plane is considered.
- The method of images leads to precise description of the radiation in this case. The integration in the resulting formulae can be easily performed numerically.
- The method can be also applied to relativistic incident particle, but only for the radiation produced from the short part of the particle's trajectory near the top of the (hemi)sphere in the particular case of extremely close fly of the particle by the (hemi)sphere top.